PAPER • **OPEN ACCESS**

Design of head-pursuit guidance law based on sliding mode control

To cite this article: Chenqi Zhu and Dejun Mu 2019 *IOP Conf. Ser.: Mater. Sci. Eng.* **563** 042076

View the article online for updates and enhancements.



IOP ebooks™

Bringing you innovative digital publishing with leading voices to create your essential collection of books in STEM research.

Start exploring the collection - download the first chapter of every title for free.

This content was downloaded from IP address 113.78.254.205 on 19/09/2019 at 11:02

IOP Conf. Series: Materials Science and Engineering **563** (2019) 042076 doi:10.1088/1757-899X/563/4/042076

Design of head-pursuit guidance law based on sliding mode control

Chenqi Zhu, Dejun Mu

Northwestern Polytechnical University, Xi'an 710072, China

15036501865@163.com

Abstract. This paper proposes a new head-pursuit guidance law based on sliding mode control to intercept hypersonic vehicle in terminal phase. In order to alleviate chattering phenomenon caused by sliding mode control and ensure the convergence speed, the combination of linear sliding variable and fast power reaching law is adopted. Furthermore, an adaptive sliding mode guidance law is designed for solving the problem of unknown upper bound of the disturbance. Also, these algorithms are proved by the theoretical perspective based on finite-time convergence theory. Finally, numerical simulations are presented to illustrate the correctness and effectiveness of the methods.

1. Introduction

Hypersonic vehicle has the characteristics of long flight distance, high flight speed and high maneuverability, which has great military value and also presents great challenges to the interception of such aircraft. As the first condition to affect the interception accuracy, the guidance law is to be one of the most important things in the design of the anti-proximity space defense system.

To fulfill the stringent performance requirements, guidance laws based on modern control theory are proposed to insure the interception accuracy. As a traditional guidance method algorithm, the proportional navigation (PN) guidance law is one of the most widely adopted. At the same time, sliding mode guidance (SMG) law is proposed for the vehicles which are hard to intercept because the sliding mode control (SMC) theory has inherent robustness against matched uncertainty. The study by Babu et al. [1] proposed a simple SMG law. Sun et al. [2] proposed a guidance law with finite convergent time. Li et al. [3] put forward adaptive neuro-fuzzy sliding mode control guidance law with impact angle constraint. Aiming at the problem of large maneuvering target and the dynamic delay characteristics of the autopilot, Zhou and Song [4] proposed a nonsingular terminal sliding mode guidance law, improving the interception accuracy. Behnamgol et al. [5] designed a new observer-based SMG law to alleviate chattering. However, the chattering problem which caused by the using of switching function in SMC is still one of the most common handicap for applying to real applications.

At the same time, the accuracy of traditional interception strategies is getting lower for the reason of that the speed of the targets is becoming faster. To meet the requirements in traditional tail-case interception, the speed of interceptors must higher than that of the targets, and unfortunately, it is hard to be ensured with the growing speed of the aim. On the other hand, traditional head-on interception causes the relative speed to become so high that it is difficult to be deal with in terminal phase. Consequently, Golan and Shima [6] proposed a head-pursuit strategy for the first time, and based on this, a second-order SMG law was designed to intercept hypersonic targets. Xiao et al. [7] proposed an

Content from this work may be used under the terms of the Creative Commons Attribution 3.0 licence. Any further distribution of this work must maintain attribution to the author(s) and the title of the work, journal citation and DOI.
Published under licence by IOP Publishing Ltd

optimal adaptive SMG law to complete head-pursuit interception for the hypersonic targets. Si et al. [8] developed an adaptive SMG law based on head-pursuit theory for intercepting hypersonic vehicle, but the structure is too complex.

In this paper, a novel SMG law which can stabilize in the limited time is designed by combining linear sliding variable and fast power reaching law. Furthermore, an adaptive SMG law is designed for solving the problem of unknown upper bound of the target. These can ensure the convergence speed and weaken the chattering phenomenon caused by sliding mode control.

2. Problem formulation

As shown in Figure 1, the head- pursuit interception against hypersonic vehicle can be divided into three stages, namely, approximation stage, orbit change stage and terminal guidance stage. First, the interceptor approaches to the goal head-on after detecting the target. Then the rail control engine of the interceptor is used to change the trajectory at the predetermined time and position, so that the interceptor is consistent with the target's flight direction and reaches the expected orbit. Finally, the interceptor enters the terminal guidance stage and adjusts the trajectory through the guidance law, making sure that the target collides with the interceptor from the back.

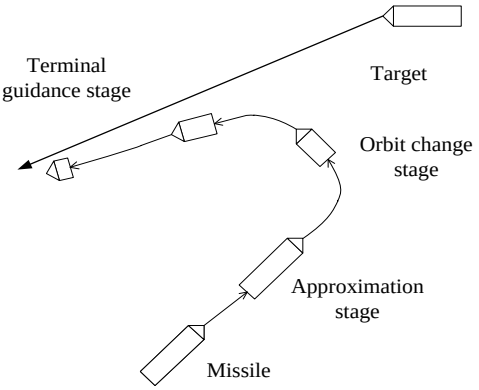


Figure 1. Head-pursuit interception schematic

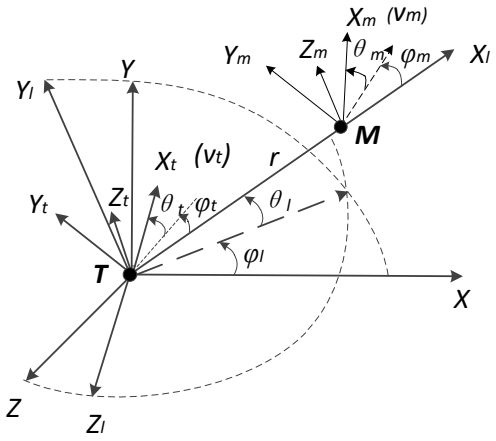


Figure 2. Three-dimensional engagement geometry

Consider a three-dimensional interceptor and target engagement as shown in Figure 2. *T* is the target and *M* is the interceptor, *T-XYZ* is inertial coordinate system (ICS), $T\text{-}X_tY_tZ_t$ is target velocity coordinate system (TVCS) of the and $T\text{-}X_mY_mZ_m$ is missile velocity coordinate system (MVCS), $T\text{-}X_lY_lZ_l$ is line-of-sight coordinate system (LCS). The LCS is converted from the ICS by rotating φ_l angle around z axis and then θ_l angle around y axis counterclockwise, the TVCS is converted from the LCS by rotating φ_t angle around z axis and then θ_t angle around y axis counterclockwise, and the MVCS is converted from the LCS by rotating φ_m angle around z axis and then θ_m angle around y axis counterclockwise, r is the relative range between missile and target, v_m and v_t represent the missile and target velocities respectively, a_{ym}, a_{zm}, a_{yt} and a_{zt} represent the missile and target accelerations which perpendicular to the direction of velocity respectively. And then the model shown in Figure 2 can be described by the following nonlinear differential equations.

$$\dot{r} = v_m \cos\theta_m \cos\varphi_m - v_t \cos\theta_t \cos\varphi_t \tag{1}$$

$$\dot{\theta}_l = \frac{v_m sin\theta_m - v_t sin\theta_t}{r} \tag{2}$$

$$\dot{\varphi}_l = \frac{v_m cos\theta_m sin\varphi_m - v_t cos\theta_t sin\varphi_t}{r cos\theta_l} \tag{3}$$

$$\dot{\theta}_t = \frac{a_{yt}}{v_t} - \dot{\varphi}_l \, sin\theta_l \sin\varphi_t - \dot{\theta}_l \, cos\varphi_t \tag{4}$$

$$\dot{\varphi}_t = -\frac{a_{zt}}{v_t cos\theta_t} + \dot{\varphi}_l \, sin\theta_l cos\varphi_t tan\theta_t - \dot{\theta}_l \sin\varphi_t tan\theta_t - \dot{\varphi}_l \, cos\theta_l \tag{5}$$

$$\dot{\theta}_m = \frac{a_{ym}}{v_m} - \dot{\varphi}_l \, sin\theta_l \sin\varphi_m - \dot{\theta}_l \, cos\varphi_m \tag{6}$$

$$\dot{\varphi}_m = -\frac{a_{zm}}{v_m cos\theta_m} + \dot{\varphi}_l \, sin\theta_l cos\varphi_m tan\theta_m - \dot{\theta}_l \sin\varphi_m tan\theta_m - \dot{\varphi}_l \, cos\theta_l \tag{7}$$

Ge and Shen [9] make the following points: Based on the analysis of the head-pursuit interception, it can be concluded that the success of head-pursuit interception requires not only r=0 at the collision point, but also the following conditions.

1） Velocity condition：

$$K = \frac{v_m}{v_t} < 1 \tag{8}$$

2） Guidance coefficient conditions：

$$\varphi_m = n_1 \varphi_t ; \quad \theta_m = n_2 \theta_t \tag{9}$$

$$n_1 > \frac{1}{K}; \qquad n_2 > \frac{1}{K} \tag{10}$$

3） Angle conditions：

$$|\theta_t| < \left(6\frac{Kn_2 - 1}{Kn_2^3 - 1} \right)^{1/2}; \qquad |\varphi_t| < \left(6\frac{Kn_1 - 1}{Kn_1^3 - 1} \right)^{1/2} \tag{11}$$

$$|\theta_m| < n_2 \left(6\frac{Kn_2 - 1}{Kn_2^3 - 1} \right)^{1/2}; \qquad |\varphi_m| < n_1 \left(6\frac{Kn_1 - 1}{Kn_1^3 - 1} \right)^{1/2} \tag{12}$$

$$\lim_{r\to 0} \varphi_m = 0; \quad \lim_{r\to 0} \varphi_t = 0; \quad \lim_{r\to 0} \theta_m = 0; \quad \lim_{r\to 0} \theta_t = 0 \tag{13}$$

3. Head-pursuit Guidance Law Design

The design of SMG law can be divided into two phases which are reaching phase (RP) and sliding mode phase (SMP). The convergence of SMP has been proved [9], therefore, only the convergence of the first stage is studied here.

In this section, some lemmas are introduced for the coming parts firstly, and then a sliding mode guidance law based on fast power approach law is designed. Furthermore, an adaptive sliding mode guidance law is designed to deal with unknown upper bound of target maneuver. The limited time stability of these two methods is proved in this section.

3.1. Lemma introduction

Lemma 1 [10]**.** Consider a nonlinear system in the form of $\dot{s} = -k_1 s - k_2 sig^{\rho}(s)$, where, k_1, $k_2 > 0$, $\rho \in (0, 1)$. Then s and $\dot{s}$ stabilizes within a limited time T which depends on initial conditions and satisfies the following equality:

$$T\left(s(0)\right)=\frac{\ln\left(1+\frac{k_1}{k_2}\left|s(0)\right|^{1-\rho}\right)}{k_1(1-\rho)} \tag{14}$$

Lemma 2 [11]**.** Supposing $b_1, b_2, \ldots b_n$, and $0 < q < 1$ are all positive numbers; then the following inequality holds:

$$\left(|b_1|+\cdots+|b_n|\right)^q \le |b_1|^q+\cdots+|b_n|^q \tag{15}$$

Lemma 3 [11]**.** Consider a nonlinear system in the form of $\dot{x}=f(x,t), x\in R^n$, if a continuous, positive-definite function $\boldsymbol{V}(x)$ satisfies the following differential inequality:

$$\dot{V}(x)+\mu V(x)+\lambda V^{\alpha}(x)\le 0 \tag{16}$$

Where, $\mu,\ \lambda>0,\ 0<\alpha<1$ are constants, and $x(t_0)=x_0,\ t_0$ is the initial time. Then, the system stabilizes within a limited time T which satisfies the following inequality:

$$T\le\frac{1}{\mu(1-\alpha)}ln\frac{\mu V^{(1-\alpha)}(x_0)+\lambda}{\lambda} \tag{17}$$

3.2. SMG law based on fast power approach law design

Based on the previous description of the head pursuit interception, the relative kinematics equations are rewritten as follows:

$$\dot{\boldsymbol{X}}=\boldsymbol{f}(\boldsymbol{X},t)+\boldsymbol{g}_1(\boldsymbol{X},t)\boldsymbol{U}(t)+\boldsymbol{g}_2(\boldsymbol{X},t)\boldsymbol{W}(t) \tag{18}$$

Where, $\boldsymbol{X}$ is the system state, $\boldsymbol{U}$ is the control input, and $\boldsymbol{W}$ is the target maneuver, and they have the following forms:

$$\boldsymbol{X}=\begin{bmatrix}\theta_m & \varphi_m & \theta_t & \varphi_t\end{bmatrix}^T;\ \boldsymbol{U}=\begin{bmatrix}u_1 & u_2\end{bmatrix}^T=\begin{bmatrix}a_{ym} & -a_{zm}\end{bmatrix}^T;$$

$$\boldsymbol{W}=\begin{bmatrix}w_1 & w_2\end{bmatrix}^T=\begin{bmatrix}\frac{a_{yt}}{v_t} & -\frac{a_{zt}}{v_t cos\theta_t}\end{bmatrix}^T;$$

$$\boldsymbol{f}(\boldsymbol{X},t)=\begin{bmatrix}-\dot{\varphi}_l sin\theta_l sin\varphi_m-\dot{\theta}_l cos\varphi_m\\ \dot{\varphi}_l sin\theta_l cos\varphi_m tan\theta_m-\dot{\theta}_l sin\varphi_m tan\theta_m-\dot{\varphi}_l cos\theta_l\\ -\dot{\varphi}_l sin\theta_l sin\varphi_t-\dot{\theta}_l cos\varphi_t\\ \dot{\varphi}_l sin\theta_l cos\varphi_t tan\theta_t-\dot{\theta}_l sin\varphi_t tan\theta_t-\dot{\varphi}_l cos\theta_l\end{bmatrix};$$

$$\boldsymbol{g}_1(\boldsymbol{X},t)=\begin{bmatrix}\frac{1}{v_m} & 0\\ 0 & \frac{1}{v_m cos\theta_m}\\ 0 & 0\\ 0 & 0\end{bmatrix};\quad \boldsymbol{g}_2(\boldsymbol{X},t)=\begin{bmatrix}0 & 0\\ 0 & 0\\ 1 & 0\\ 0 & 1\end{bmatrix};$$

Then, the following forms of linear sliding mode variable and fast power approach law are designed:

$$\boldsymbol{S}=\begin{bmatrix}s_1 & s_2\end{bmatrix}^T=\boldsymbol{CX} \tag{19}$$

$$\dot{\boldsymbol{S}}=-k_1\boldsymbol{S}-k_2 sig^{\rho}(\boldsymbol{S}) \tag{20}$$

Where

$$\boldsymbol{C}=\begin{bmatrix}1 & 0 & -n_1 & 0\\ 0 & 1 & 0 & -n_2\end{bmatrix},\quad sig^{\rho}(\boldsymbol{S})=\begin{bmatrix}|s_1|^{\rho}\,sign(s_1)\\ |s_2|^{\rho}\,sign(s_2)\end{bmatrix};n_1、\ n_2>0,\ \ k_1、\ k_2>0,\ \ \rho\in(0,1)$$

Theorem 1.

Consider a nonlinear system in the form of formula (18), by adopting the sliding variable as equation (19) and using the control input

$$\boldsymbol{U}=-\left[\boldsymbol{Cg}_1(\boldsymbol{X},t)\right]^{-1}\left[\boldsymbol{Cf}(\boldsymbol{X},t)+k_1\boldsymbol{S}+\boldsymbol{Cg}_2(\boldsymbol{X},t)\boldsymbol{W}(t)+k_2 sig^{\rho}(\boldsymbol{S})\right] \tag{21}$$

The sliding variable $\boldsymbol{S}$ will converge within finite reaching time.

Proof.

Substituting equation (21) in (19) and taking the derivative of the result yields

$$\dot{\boldsymbol{S}}=-k_1\boldsymbol{S}-k_2 sig^{\rho}(\boldsymbol{S}) \tag{22}$$

According to the lemma 1, the sliding variable $\boldsymbol{S}$ stabilizes within a limited time.

Theorem 2.

Consider a nonlinear system in the form of formula (18), assuming $\boldsymbol{W}$ has a band with the forms:$|w_1|<\varepsilon_1$, $|w_2|<\varepsilon_2$, where, ε_1, ε_2 are positive numbers. By adopting the sliding variable as equation (19) and using the control input

$$\boldsymbol{U}_1=-\left[\boldsymbol{Cg}_1(\boldsymbol{X},t)\right]^{-1}\left[\boldsymbol{Cf}(\boldsymbol{X},t)+k_1\boldsymbol{S}+k_2 sig^{\rho}(\boldsymbol{S})-\boldsymbol{Cg}_2(\boldsymbol{X},t)\sigma sign(\boldsymbol{S})\right] \tag{23}$$

Where

$$\boldsymbol{C}=\begin{bmatrix}1 & 0 & -n_1 & 0\\ 0 & 1 & 0 & -n_2\end{bmatrix},\ sig^{\rho}(\boldsymbol{S})=\begin{bmatrix}|s_1|^{\rho}\,sign(s_1)\\ |s_2|^{\rho}\,sign(s_2)\end{bmatrix},$$

$$n_1,\ n_2>0,\ k_1,\ k_2>0,\ \sigma>\max(\varepsilon_1,\ \varepsilon_2),\ \rho\in(0,1)$$

The sliding variable $\boldsymbol{S}$ will converge in finite reaching time.

Proof.

Defining a Lyapunov function $\boldsymbol{V}_1$ as follows

$$V_1=\frac{1}{2}S^TS \tag{24}$$

Then, taking the derivative of $\boldsymbol{V}_1$

$$\begin{aligned}\dot{V}_1&=S^T[-k_1S-k_2sig^{\rho}(S)+Cg_2(X,t)\sigma sign(S)+Cg_2(X,t)W(t)]\\&=-k_1S^TS-k_2S^Tsig^{\rho}(S)+S^TCg_2(X,t)W(t)+S^TCg_2(X,t)\sigma sign(S)\\&=-k_1S^TS-k_2S^Tsig^{\rho}(S)+(-s_1w_1n_1-s_2w_2n_2)+(-|s_1|\delta n_1-|s_2|\delta n_2)\\&\le-k_1S^TS-k_2S^Tsig^{\rho}(S)+(|s_1||w_1|n_1+|s_2||w_2|n_2)-(|s_1|\delta n_1+|s_2|\delta n_2)\\&\le-k_1S^TS-k_2S^Tsig^{\rho}(S)+(|s_1||w_1|n_1-|s_1|\delta n_1)+(|s_2||w_2|n_2-|s_2|\delta n_2)\\&\le-k_1S^TS-k_2S^Tsig^{\rho}(S)\end{aligned}$$

where

$$\boldsymbol{S}^Tsig^{\rho}(\boldsymbol{S})=|s_1|^{\rho+1}+|s_2|^{\rho+1}=\left(s_1^2\right)^{\frac{\rho+1}{2}}+\left(s_2^2\right)^{\frac{\rho+1}{2}}$$

According to the lemma 2 get the following inequality

$$\left(s_1^2\right)^{\frac{\rho+1}{2}}+\left(s_2^2\right)^{\frac{\rho+1}{2}}\ge\left(s_1^2+s_2^2\right)^{\frac{\rho+1}{2}}=(2\boldsymbol{V}_1)^{\frac{\rho+1}{2}}=2^{\frac{\rho+1}{2}}\boldsymbol{V}_1^{\frac{\rho+1}{2}}$$

Therefore, getting the following inequality

$$\dot{V}_1 \le -2k_1V_1 - 2^{\frac{\rho+1}{2}}k_2V_1^{\frac{\rho+1}{2}}$$

This implies that

$$\dot{V}_1 + 2k_1V_1 + 2^{\frac{\rho+1}{2}}k_2V_1^{\frac{\rho+1}{2}} \le 0$$

According to the lemma 3, the sliding variable $\boldsymbol{S}$ stabilizes within a limited time.

3.3. ASMG law based on fast power approach law design

Theorem 2 assumes the upper bound of target maneuver as a known parameter σ, however, the σ is difficult to be given accurately in practice. If the σ is too large, it will lead to over-control, and inversely, it will lead to system instability. Therefore, theorem 2 needs to be improved to deal with the unknown upper bound of target maneuver.

Regarding the unknown upper bound of target maneuver as a function of time, then, $\varepsilon = \begin{bmatrix}\varepsilon_1 & \varepsilon_2\end{bmatrix}^T$, $\breve{\varepsilon} = \varepsilon - \hat{\varepsilon} = \begin{bmatrix}\breve{\varepsilon}_1 & \breve{\varepsilon}_2\end{bmatrix}^T$, where, $\boldsymbol{\varepsilon}$ is the unknown upper bound, $\hat{\boldsymbol{\varepsilon}}$ is an estimate of $\boldsymbol{\varepsilon}$, $\breve{\boldsymbol{\varepsilon}}$ is error of estimation.

Theorem 3.

Consider a nonlinear system in the form of formula (18), assuming $\boldsymbol{W}$ has a unknown upper bound. By adopting the sliding variable as equation (19) and using the control input

$$\begin{aligned} \boldsymbol{U}_2 &= -\left[\boldsymbol{Cg}_1(\boldsymbol{X},t)\right]^{-1}\left[\boldsymbol{Cf}(\boldsymbol{X},t) + \boldsymbol{Cg}_2(\boldsymbol{X},t)\boldsymbol{R}\hat{\boldsymbol{\varepsilon}} + k_1\boldsymbol{S} + k_2 sig^{\rho}(\boldsymbol{S})\right] \\ \dot{\hat{\boldsymbol{\varepsilon}}} &= \gamma\left|\boldsymbol{Cg}_2(\boldsymbol{X},t)\right|^T|\boldsymbol{S}| \end{aligned} \tag{25}$$

where γ is a weighting coefficient, $\boldsymbol{R} = \begin{bmatrix} sign(s_1) & 0 \\ 0 & sign(s_2) \end{bmatrix}$, the sliding variable $\boldsymbol{S}$ will converge in finite reaching time.

Proof.

Defining a Lyapunov function $\boldsymbol{V}_2$ as follows

$$\boldsymbol{V}_2 = \frac{1}{2}\boldsymbol{S}^T\boldsymbol{S} + \frac{1}{2\gamma}\tilde{\boldsymbol{\varepsilon}}^T\tilde{\boldsymbol{\varepsilon}} \tag{26}$$

Where, $\tilde{\boldsymbol{\varepsilon}} = \boldsymbol{\varepsilon} - \hat{\boldsymbol{\varepsilon}} = \begin{bmatrix}\boldsymbol{\varepsilon}_1 & \boldsymbol{\varepsilon}_2\end{bmatrix}^T$. Taking the derivative of $\boldsymbol{V}_1$ yields

$$\begin{aligned} \dot{\boldsymbol{V}}_2 &= -\boldsymbol{k}_1\boldsymbol{S}^T\boldsymbol{S} - \boldsymbol{k}_2\boldsymbol{S}^T sig^{\rho}(\boldsymbol{S}) + \boldsymbol{S}^T\boldsymbol{Cg}_2(\boldsymbol{X},t)\boldsymbol{W}(\boldsymbol{t}) - \boldsymbol{S}^T\boldsymbol{Cg}_2(\boldsymbol{X},t)\boldsymbol{R}\hat{\varepsilon} - \frac{1}{\gamma}\tilde{\varepsilon}^T\dot{\hat{\varepsilon}} \\ &\le -\boldsymbol{k}_1\boldsymbol{S}^T\boldsymbol{S} - \boldsymbol{k}_2\boldsymbol{S}^T sig^{\rho}(\boldsymbol{S}) + |\boldsymbol{S}|^T\left|\boldsymbol{Cg}_2(\boldsymbol{X},\boldsymbol{t})\right|\varepsilon - \boldsymbol{S}^T\boldsymbol{Cg}_2(\boldsymbol{X},\boldsymbol{t})\boldsymbol{R}\hat{\varepsilon} - \frac{1}{\gamma}\tilde{\varepsilon}^T\dot{\hat{\varepsilon}} \\ &= -\boldsymbol{k}_1\boldsymbol{S}^T\boldsymbol{S} - \boldsymbol{k}_2\boldsymbol{S}^T sig^{\rho}(\boldsymbol{S}) + |\boldsymbol{S}|^T\left|\boldsymbol{Cg}_2(\boldsymbol{X},\boldsymbol{t})\right|\varepsilon - |\boldsymbol{S}|^T\left|\boldsymbol{Cg}_2(\boldsymbol{X},\boldsymbol{t})\right|\hat{\varepsilon} - \frac{1}{\gamma}\tilde{\varepsilon}^T\dot{\hat{\varepsilon}} \\ &= -\boldsymbol{k}_1\boldsymbol{S}^T\boldsymbol{S} - \boldsymbol{k}_2\boldsymbol{S}^T sig^{\rho}(\boldsymbol{S}) + |\boldsymbol{S}|^T\left|\boldsymbol{Cg}_2(\boldsymbol{X},\boldsymbol{t})\right|(\varepsilon - \hat{\varepsilon}) - \frac{1}{\gamma}\tilde{\varepsilon}^T\dot{\hat{\varepsilon}} \\ &= -\boldsymbol{k}_1\boldsymbol{S}^T\boldsymbol{S} - \boldsymbol{k}_2\boldsymbol{S}^T sig^{\rho}(\boldsymbol{S}) + |\boldsymbol{S}|^T\left|\boldsymbol{Cg}_2(\boldsymbol{X},\boldsymbol{t})\right|\tilde{\varepsilon} - \frac{1}{\gamma}\tilde{\varepsilon}^T\dot{\hat{\varepsilon}} \\ &= -\boldsymbol{k}_1\boldsymbol{S}^T\boldsymbol{S} - \boldsymbol{k}_2\boldsymbol{S}^T sig^{\rho}(\boldsymbol{S}) + \tilde{\varepsilon}^T\left|\boldsymbol{Cg}_2(\boldsymbol{X},\boldsymbol{t})\right|^T|\boldsymbol{S}| - \frac{1}{\gamma}\tilde{\varepsilon}^T\dot{\hat{\varepsilon}} \\ &= -\boldsymbol{k}_1\boldsymbol{S}^T\boldsymbol{S} - \boldsymbol{k}_2\boldsymbol{S}^T sig^{\rho}(\boldsymbol{S}) \end{aligned}$$

$$\leq -2\boldsymbol{k}_1\boldsymbol{V}_2 - 2^{\frac{\rho+1}{2}}\boldsymbol{k}_2\boldsymbol{V}_2^{\frac{\rho+1}{2}}$$

This implies that

$$\dot{\boldsymbol{V}}_2 + 2k_1\boldsymbol{V}_2 + 2^{\frac{\rho+1}{2}}k_2\boldsymbol{V}_2^{\frac{\rho+1}{2}} \leq 0$$

According to the Lemma 3, the sliding variable $\boldsymbol{S}$ stabilizes within a limited time.

4. Numerical simulation

In this section, the effectiveness and correctness of the guidance laws designed in this paper is demonstrated by several numerical simulations compering with the double-power reaching laws.

We consider the situation in which the initial relative range between missile and target is 7500m, the initial missile coordinate is (7224.6, -1535.7, -1302.3) and the target is (0, 0, 0), the initial missile and target velocities are $\boldsymbol{V}_{\mathrm{m}}$=1500m/s, $\boldsymbol{V}_{\mathrm{t}}$=2100m/s respectively, the initial line-of-sight angles are $\theta_{l0}=-10^{\circ}$, $\varphi_{l0}=-12^{\circ}$, initial missile lead angles are $\theta_{m0}=-20^{\circ}$, $\varphi_{m0}=-15^{\circ}$ and the target $\theta_{t0}=-20^{\circ}$, $\varphi_{t0}=-15^{\circ}$, the acceleration of the target is 2g.These values are all the same in following numerical simulation cases.

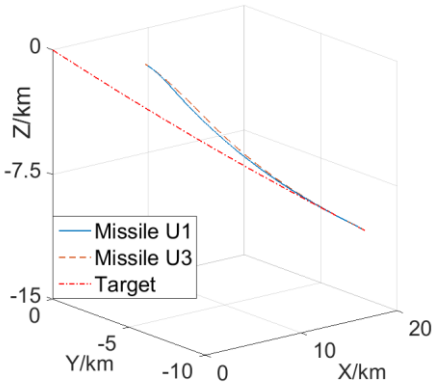


Figure 3. Relative motion orbit

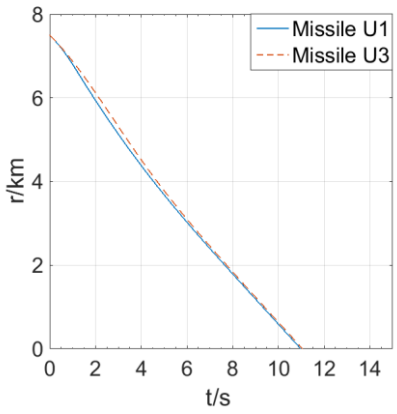


Figure 4. Relative range between missile and target

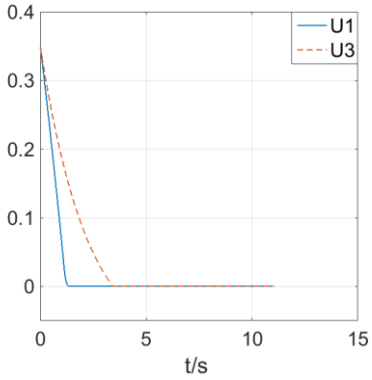


Figure 5. Sliding mode variable s_1

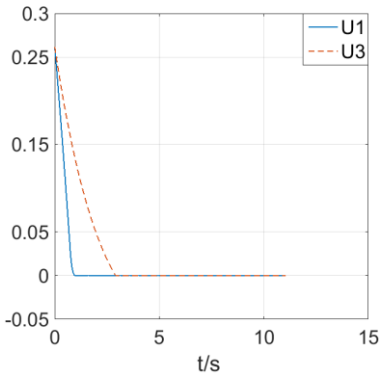


Figure 6. Sliding mode variable s_2

4.1. Verify U_1

This case presents the simulation results of intercepting maneuvering targets with known upper bounds, the parameters in equation (23) are designed as $\delta = 0.05$, $n_1 = n_2 = 2$, $k_1 = 10$, $k_2 = 0.4$, $\rho = 0.9$.

Choosing the double-power reaching law as follows

$$\boldsymbol{U}_3 = -\left[\boldsymbol{Cg}_1(\boldsymbol{X},t)\right]^{-1}\left[\boldsymbol{Cf}(\boldsymbol{X},t) - \boldsymbol{Cg}_2(\boldsymbol{X},t)\sigma sign(\boldsymbol{S}) + k_3 sig^{\alpha}(\boldsymbol{S}) + k_2 sig^{\rho}(\boldsymbol{S})\right] \tag{27}$$

Where, $k_3 = 1$, $\alpha = 5$. The simulation results are shown in figures 3~10.

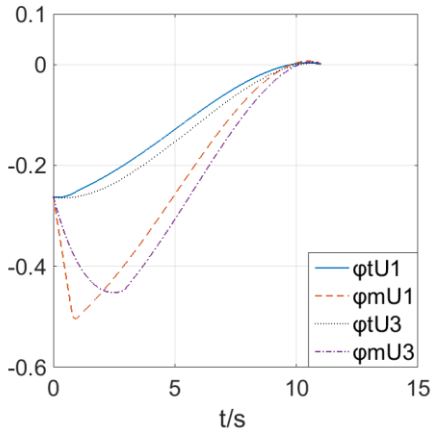


Figure 7. Lead angle θ

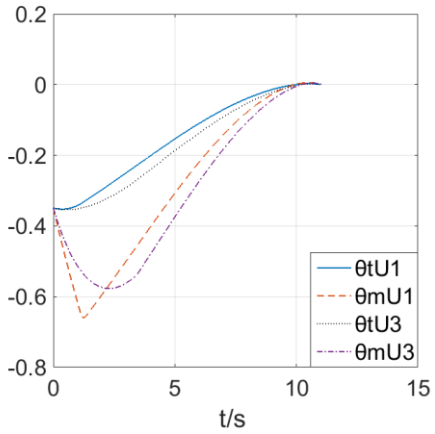


Figure 8. Lead angle φ

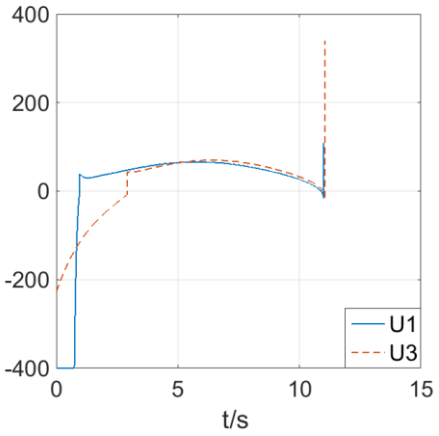


Figure 9. Missile acceleration a_{ym}

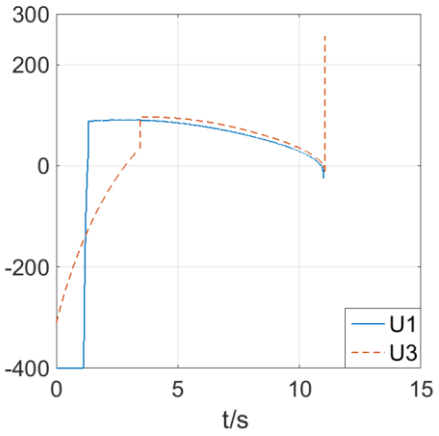


Figure 10. Missile acceleration $\boldsymbol{a}_{zm}$

Figure 3 shows the relative motion orbit of the missile and target by using the SMG law U_1 and U_3. Figure 4 shows the relative range between missile and target. The results indicate that U_1 and U_3 both can intercept the target in a similar trajectory within 12s. Figure 5 and Figure 6 show the sliding mode variables of the missile and target by using SMG law U_1 and U_3, and the results demonstrate that, the SMG law designed in this paper has a faster convergence rate. Figure 7 shows lead angle θ and Figure 8 shows lead angle φ by using SMG law U_1 and U_3, respectively, the results indicate the two laws both can make sure that the θm and φm keep twice times the θt and φt after 3s and converge to 0 synchronously. Figure 9 and Figure 10 show the missile acceleration aym and azm , the result manifest that the two guidance laws have a similar overload capability requirements for the missile, and there is no obvious chattering phenomenon.

Based on the above analysis, it can be obtained that the guidance law designed in this paper has a faster convergence speed on the basis of weakening chattering..

4.2. Verify U_2

This case presents the simulation results of intercepting maneuvering targets with known upper bounds, the parameters in equation (23) are designed asγ=0.02，n_1=n_2=2，k_1=10，k_2=0.4，ρ=0.9，Choosing an adaptive double-power reaching law as follows

$$\boldsymbol{U}_4 = -\left[\boldsymbol{Cg}_1\left(\boldsymbol{X},t\right)\right]^{-1}\left[\boldsymbol{Cf}\left(\boldsymbol{X},t\right) - \boldsymbol{Cg}_2\left(\boldsymbol{X},t\right)\boldsymbol{R}\hat{\boldsymbol{\varepsilon}} + k_3 sig^{\alpha}\left(\boldsymbol{S}\right) + k_2 sig^{\rho}\left(\boldsymbol{S}\right)\right] \tag{28}$$

Where, $k_3 = 1$, $k_4 = 0.01$, $\alpha = 5$, the simulation results are shown in figures 11~18.

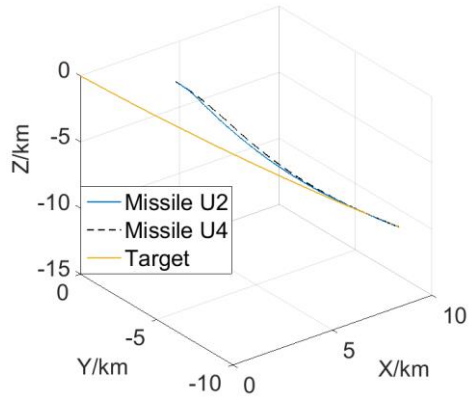


Figure 11. Relative motion orbit

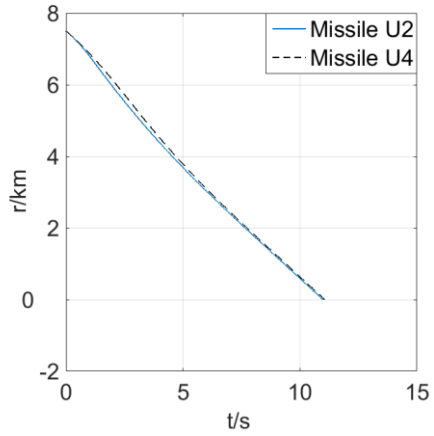


Figure 12. Relative range between missile and target

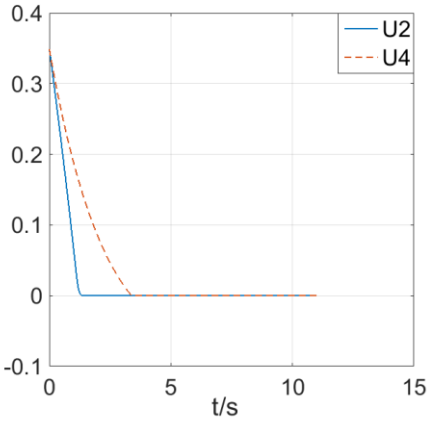


Figure 13. Sliding mode surface s_1

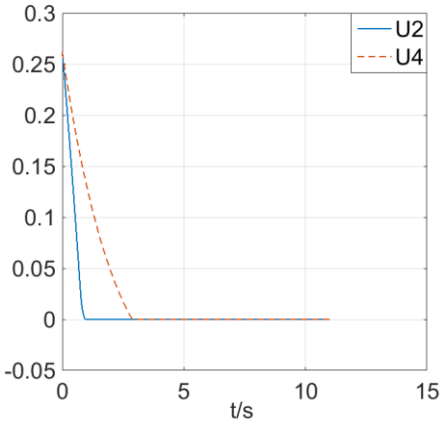


Figure 14. Sliding mode surface s_2

Similar to previous section, Figure 11 and Figure 12 show the relative motion orbit and relative range by using adaptive SMG law U_2 based on fast power approach law and adaptive SMG law U_4 based on double power approach law guidance law, respectively. The results indicate that U_2 and U_4 both can intercept the target in a similar trajectory. Figure 13 and Figure 14 show the sliding mode surfaces of the missile and target by using SMG law U_2 and U4, and the results demonstrate that, the adaptive SMG law designed in this paper has a faster convergence rate. Figure 15 and Figure 16 show the lead angle θ and φ by using adaptive SMG law U_2 and U_4, respectively, the results indicate that U_2 and U_4 both can

satisfy the guidance coefficient conditions. Figure 17 and Figure 18 show the missile acceleration aym and azm, the result manifest that the overload capability requirements for the missile are similar in the case of the two adaptive laws, and there is no obvious chattering.

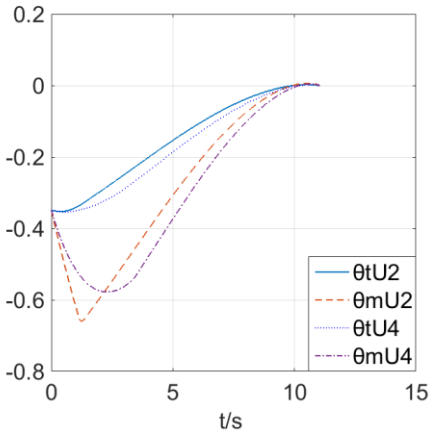


Figure 15. Lead angle θ

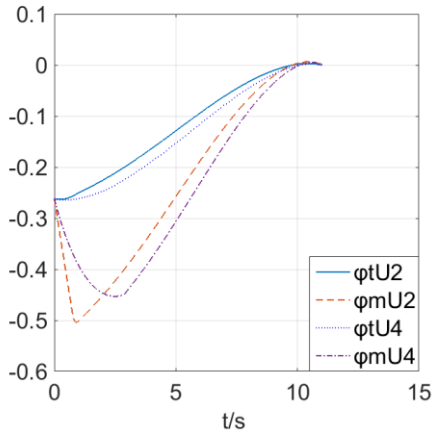


Figure 16. Lead angle φ

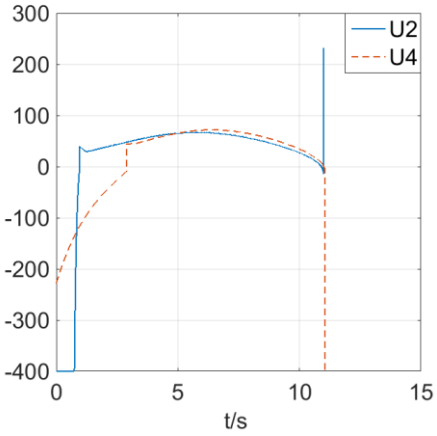


Figure 17. Missile acceleration a_{ym}

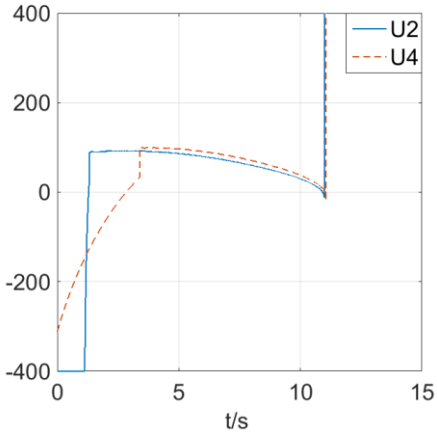


Figure 18. Missile acceleration a_{zm}

It can be proved that the guidance law U_2 can accelerate the convergence speed on the basis of weakening chattering, although in the case of unknown upper bound of the target maneuver

5. Conclusion

The new SMG laws are designed. The structures of the proposed guidance laws are developed based on fast power reaching law. The stabilizations of the guidance laws are proved by the theoretical perspective based on finite-time convergence theory, and the correctness and effectiveness of the theories are verified by numerical simulation.

References

[1] Babu K R, Sarma I G and Swamy K N, 1994 Switched bias proportional navigation for homing guidance against highly maneuvering targets. *J. Guid Control Dynam* **17 6** p. 1357-63.

[2] Sun L, Wang W, Yi R, Xiong S, 2016 A novel guidance law using fast terminal sliding mode control with impact angle constraints. *ISA T* **64 2016** p. 12-23.

[3] Li Q, Zhang W, Han G and Yang Y, 2015 Adaptive neuro-fuzzy sliding mode control guidance law with impact angle constraint *Iet Control Theory A* **9 14** p. 2115-23.
[4] Zhou H B and Song J H, 2018 Sliding Mode Guidance Law Considering Missile Dynamic Characteristics and Impact Angle Constraints *IJAC* **15 2** p. 218-28.
[5] Behnamgol V, Vali A R and Mohammadi A, 2015 A new observer-based chattering-free sliding mode guidance law. *P I Mech Eng G-J Aer* **230 8** p. 1486-95.
[6] Golan O and Shima T, 2004 Head Pursuit Guidance for Hypervelocity Interception. *NCC CP-4885 AIAA 2004* Washington p.1-12.
[7] Xiao K, Sun B, Zhang W, Cai Y, 2013 Head Pursuit Optimal Adaptive Sliding Mode Guidance Law. *IFAC Proceedings Volumes* **46 13** p. 508-13.
[8] Si, Y J, Song, S M and Wei X Q, 2017 An adaptive reaching law based three-dimensional guidance laws for intercepting hypersonic vehicle *IJICIC* **13 4** p. 1335-49.
[9] Ge, L Z. and Shen, Y, 2008 Head pursuit variable structure guidance law for three-dimensional space interception *Chinese J Aeronaut* **21 3** p. 247-51
[10] Yu S, Yu X, Shirinzadeh B and Man Z, 2005 Continuous finite-time control for robotic manipulators with terminal sliding mode. *Automatica* **41 11** p. 1957-64.
[11] Liu K P, CaoY M, Wang S Q and Li Y C, 2015 Terminal sliding mode control for landing on asteroids based on double power reaching law *2015 IEEE ICIA* p. 2444-49.